Optical Materials: X 16 (2022) 100210

Contents lists available at ScienceDirect

Optical Materials: X

journal homepage: www.journals.elsevier.com/optical-materials-x

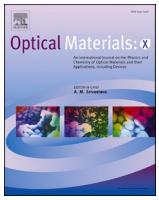

Low temperature thermoluminescence of β-Ga_2O_3 scintillator

Marcin E. Witkowski [a,*], Konrad J. Drozdowski [a], Michał Makowski [a], Winicjusz Drozdowski [a], Andrzej J. Wojtowicz [a], Klaus Irmscher [b], Robert Schewski [b], Zbigniew Galazka [b]

[a] Institute of Physics, Faculty of Physics, Astronomy and Informatics, Nicolaus Copernicus University in Toruń, ul, Grudziądzka 5, 87-100, Toruń, Poland
[b] Leibniz-Institut für Kristallzüchtung, Max-Born-Str. 2, 12489, Berlin, Germany

ARTICLE INFO

Keywords:
β-Ga_2O_3 crystal
Czochralski method
Low temperature thermoluminescence
Traps

ABSTRACT

Low temperature thermoluminescence of β-Ga_2O_3, β-Ga_2O_3:Al and β-Ga_2O_3:Ce has been investigated. Glow curves have been analyzed quantitatively using a rate equations model in order to determine the traps parameters, such as activation energies, capture cross-sections and probabilities of recombination and retrapping.

1. Introduction

Although the present scintillator market is completely dominated by inorganic insulators, some semiconductors are at least considered by scientists as potential fast and bright scintillators [1]. One of the most promising candidates, β-Ga_2O_3 with a density of 5.96 g/cm^{-3} and a bandgap of 4.85 eV, has recently been studied intensively by various scientific groups [2–8]. Although diverse dopants have been examined, according to the most recent reports it is undoped β-Ga_2O_3 crystal that displays the highest scintillation light output, based on its intrinsic luminescence, while for making its scintillation faster some Si doping is necessary (in fact, both light yield and scintillation decay times are driven by the free electron concentration and, unfortunately, anti-correlate with each other, i.e. the higher the yield the slower the scintillation decay [7–9]).

Despite a variety of reports on β-Ga_2O_3 available in the literature, there is hardly any information about thermoluminescence (TL) of this material. There are only three preceding papers. Islam et al. [10] analyzed glow curves of pure and doped β-Ga_2O_3 crystals measured in the temperature range from 227 to 677 K. They also presented TL emission spectra and ascribed the detected traps to some impurities related to the presence of Fe in the crystals. Luchechko et al. [11] studied TL of β-Ga_2O_3:Mg crystals after their exposure to X-rays at 85 K and evaluated the trap depths. However, since doping β-Ga_2O_3 crystals with Mg makes them semi-insulating [12] the only publication describing low temperature TL (ltTL) of semiconducting β-Ga_2O_3 crystals (undoped and doped) is our recent work [9]. It explains the composition of the glow spectra between 10 and 350 K on the concentration of free electrons, which determines the conductivity of the crystal:

a) for electrical insulators TL is formed by a glow peak at about 90–110 K for β-Ga_2O_3:Ce, for some samples accompanied by two more peaks at higher temperatures;
b) for normal semiconductors with low and moderate values of free electron concentration TL is dominated by a broad glow peak below 60 K;
c) for degenerate semiconductors with high values of free electron concentration no TL is observed in the entire experimental range (10–350 K).

A simple model explaining this dependence by the position of the Fermi level in the bandgap has also been included. We note, however, that these results are not complete, because no parameters of the traps have been derived.

In this Communication we continue our studies of the low temperature thermoluminescence of undoped and doped β-Ga_2O_3. We apply an extended quantitative glow curve analysis employing a model based on some specific rate equations, which let us find the parameters of all the detected traps. Some tentative interpretations are also provided.

2. Materials and experiment

High-quality bulk single crystals of β-Ga_2O_3 (either undoped or doped with Al or Ce) were grown by the Czochralski method along the <010> crystallographic direction as described in detail by Galazka et al. [8,13]. 5 × 5 mm^2 and (0.50 ± 0.05) mm thick (100) oriented crystal

* Corresponding author.
E-mail address: mwit@fizyka.umk.pl (M.E. Witkowski).

https://doi.org/10.1016/j.omx.2022.100210
Received 29 December 2021; Received in revised form 18 October 2022; Accepted 22 October 2022
Available online 12 November 2022

samples were prepared by cleaving parallel to the easy cleavage plane {100}. The list of the investigated samples, which are either electrical insulators or normal semiconductors, is presented in Table 1. The dopant concentrations are those in the melt (in mol%), while the free electron concentrations were determined by the Hall effect measurements.

Low temperature TL glow curves were recorded with a typical set-up built of an Inel X-ray generator (45 kV/10 mA), an ARC SP-500i monochromator (set to the 0^{th}-order), a Hamamatsu R928 photomultiplier, and an APD Cryogenics closed-cycle helium cooler controlled by a Lake Shore 330 unit. Before the TL runs, the samples were irradiated with X-rays at 10 K for 10 min. The heating rate was 0.145 K/s.

3. Results and discussion

The ltTL measurements have been performed on a number of crystal samples. However, based on our recent conclusions [9], for clarity of presentation we have chosen just four characteristic glow curves recorded on the samples listed in Table 1. These curves are presented in Fig. 1a–d, containing the recorded luminescence intensity as a function of time (including the steady-state luminescence during X-ray irradiation, then afterglow and thermoluminescence), as well as the heating profile (by linear fitting a heating rate of 0.145 K/s has been found for all cases, with a maximum error of 0.002 K/s). In each run, first the background is recorded for 120 s, then the sample is irradiated with X-rays for 600 s, next the afterglow signal is recorded for 2880 s, and finally the heater is switched on. Prior to the glow curve analysis, a sum of three exponential functions is used to fit the afterglow part, which is further extrapolated to the range of heating and subtracted in the next step, providing glow curves not affected by the presence of some afterglow. For such curves we have first checked the asymmetric geometry factors of all peaks. Since these factors significantly differ from the value of 0.42 characteristic for a first-order peak [14], the glow curve analysis cannot be based on the classic Randall-Wilkins approach [15].

To describe correctly all the processes contributing to the observed glow curves, we have adopted a model presented previously by McKeever et al. [16], Chen and McKeever [17], and Chen and Pagonis [18]. The energy diagram employed by the model, presented in Fig. 2, includes conduction and valence bands, several trapping levels and radiative recombination centers. The rate equations describing the excitation stage are as follows:

$$\frac{dn_i}{dt} = -p_i n_i + A_{n_i}(N_i - n_i)n_c, i = 1, 2, \ldots, l \tag{1.1}$$

$$\frac{dm_j}{dt} = -A_{r_j} n_c m_v + B_{m_j}(M_j - m_j)m_v, j = 1, 2, \ldots, k \tag{1.2}$$

$$\frac{dm_v}{dt} = X - \sum_{j=1}^{k} B_{m_j}(M_j - m_j)m_v \tag{1.3}$$

Table 1
The list of the investigated samples.

ID	formula	free electron concentration (cm^{-3})	size (mm^3)
a	β-Ga_2O_3:Al (5.0%)	insulator	5 × 5 × 0.52
b	β-Ga_2O_3:Ce (0.1%)	insulator	5 × 5 × 0.20
c	β-Ga_2O_3	insulator	5 × 5 × 0.54
d	β-Ga_2O_3	$1.5{\cdot}10^{16}$	5 × 5 × 0.57

$$\frac{dn_c}{dt} + \sum_{i=1}^{l}\frac{dn_i}{dt} = \frac{dm_v}{dt} + \sum_{j=1}^{k}\frac{dm_j}{dt} \tag{1.4}$$

where n_c (cm^{-3}) is the density of free electrons in the conduction band (CB); m_v (cm^{-3}) - the density of free holes in the valence band (VB); N_i and M_j (cm^{-3}) - the maximum possible charge densities in TL-active traps (T_i) and recombination centers (R_j), respectively; n_i and m_j (cm^{-3}) - the current occupancies of N_i and M_j levels, respectively; A_{n_i}, B_{m_j} and A_{r_j} (cm^3/s) - relevant transition probabilities: for a CB electron to become trapped in a trap, for a VB hole to become captured by a recombination center, and for a CB electron to recombine with an ionized luminescence center, respectively. Finally, p_i is defined by the formula:

$$p_i = s_i \exp\left(-\frac{E_i}{k_B T}\right) \tag{2}$$

and is the probability of electron release into the conduction band upon thermal ionization of a TL-active trap; herein E_i (eV) is the process activation energy, s_i (s^{-1}) - the frequency factor, k_B - the Boltzmann constant, and T - the temperature (which is a function of time). Moreover, it is assumed that the frequency factor is also a function of temperature and is given by the formula:

$$s_i(T) = \sigma_i(T) N_c(T) v(T) \tag{3}$$

where σ_i is the capture cross section for capturing electrons, N_c - the effective density of states at the CB edge, $<v>$ – the average thermal velocity if electrons; all these quantities are specified by the expressions:

$$\sigma_i = \sigma_\infty^i \, exp\left(-\frac{E_{q_i}}{k_B T}\right) \tag{4.1}$$

$$N_c = 2\left(\frac{2\pi m_* k_B T}{h^2}\right)^{3/2} \tag{4.2}$$

$$v \approx \sqrt{v^2} = \sqrt{\frac{3k_B T}{m_*}} \tag{4.3}$$

where m_* is the electron effective mass, E_{q_i} - the capture cross section's activation energy, and h is the Planck constant. Ultimately, based on (2), (3), and (4.1-4.3) p_i can be written as:

$$p_i = \sigma_\infty^i \, exp\left(-\frac{E_{q_i}}{k_B T}\right) 2\left(\frac{2\pi m_* k_B T}{h^2}\right)^{3/2} \sqrt{\frac{3k_B T}{m_*}} \exp\left(-\frac{E_i}{k_B T}\right) = 4\sqrt{6}\,\frac{\pi\sqrt{\pi} m_* k_B^2 T^2}{h^3}\sigma_\infty^i \exp\left(-\frac{E_i + E_{q_i}}{k_B T}\right) \tag{5}$$

We note that there is no general analytical solution for the set of equations (1.1) - (1.4). Therefore, to solve this set of equations we have introduced some assumptions and simplifications. We assume that we deal with several traps with different E_i and σ_i values and different trapping probabilities A_{n_i}, and a single recombination center (i.e. $k = 1$ in equations (1.1) - (1.4)), which is created when a valence band hole self-traps on a single oxygen ion (self-trapped hole, STH). Self-trapped holes attract and bind a conduction band electrons (free or thermally released from electron traps) creating self-trapped excitons (STE). Decaying STE emit UV photons. Since we are interested in the time range after the X-ray irradiation, we put $X = 0$. Moreover, since the mobility of holes is significantly smaller than the mobility of electrons in β-Ga_2O_3, we approximate $dm_v/dt \approx 0$.

For each glow curve we have put initial parameters into the set of

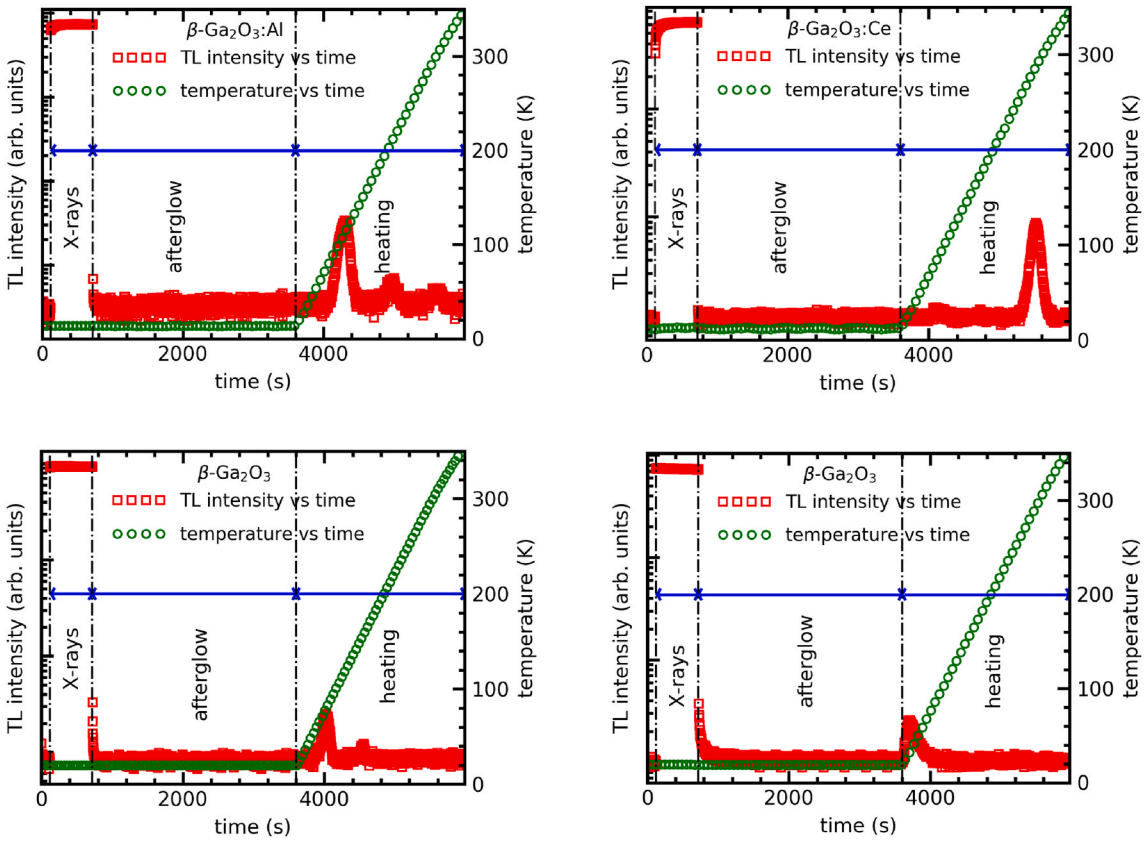

Fig. 1. Full thermoluminesecence readout for all the samples from Table 1 (red squares - luminescence intensity, green circles - heating profile). (For interpretation of the references to colour in this figure legend, the reader is referred to the Web version of this article.)

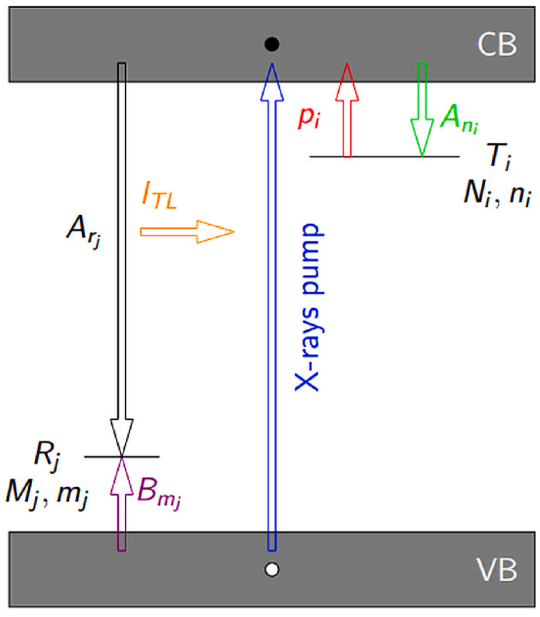

Fig. 2. A scheme of the employed model.

equations (1.1) - (1.4). Next, we have launched a fit using the nonlinear least-squares Levenberg-Marquardt method [19,20]. A fitting program employing the set of rate equations has been written in Python 3.7 with *odeint* package from SciPy extension.

The resultant fitted curves together with the derived trap parameters are shown in Fig. 3a–d and Table 2. We have also calculated the following ratios:

$$f_i = \frac{n_{0,i}}{N_i} \tag{6.1}$$

$$R_i = \frac{A_{n_i}}{A_{r_j}} \tag{6.2}$$

representing the initial filling and the relation between retrapping and recombination, respectively.

For discussing the glow curves we refer to traps already reported for β-Ga_2O_3 (measured by the deep-level transient spectroscopy, deep-level optical spectroscopy, thermally stimulated current, photoinduced current transient spectroscopy, steady-state photo-capacitance spectroscopy, and micro-cathodoluminescence), the distribution and particularly concentrations of which differ in bulk single crystals and thin films, as summarized by Zhang et al. [21], Nakano [22] and Galazka [5]. Bulk crystals grown from the melt contained within an Ir crucible (Czochralski and EFG methods) have a number of residual impurities (typically at a level of single wt. ppm) arising from the metal crucible, starting material, and thermal insulation. The mostly occurring impurities in the Czochralski-grown crystals are Fe, Co, Ir, Al, Zr, Ca and Si [23], with some of them acting as trapping centers. There are several traps found in the melt-grown β-Ga_2O_3 that are distributed over the whole energy gap with typical concentrations of about 10^{14}-10^{16} cm^{-3}. On the other hand, typical trap concentration in β-Ga_2O_3 films is about two orders of magnitude lower. Energetically, the traps in the Czochralski and/or EFG-grown crystals are typically located at 0.55–0.62 (E1), 0.74–0.82 (E2), 1.00–1.04 (E3), 1.48 (E4), 2.16 (E5), and 4.4 (E6) eV below the conduction band, with dominating E2 trap (note the deep trap levels may differ to some extent depending on the technique). Some of the traps have been assigned to Fe, Co, Ir, and Mg impurities [24–27],

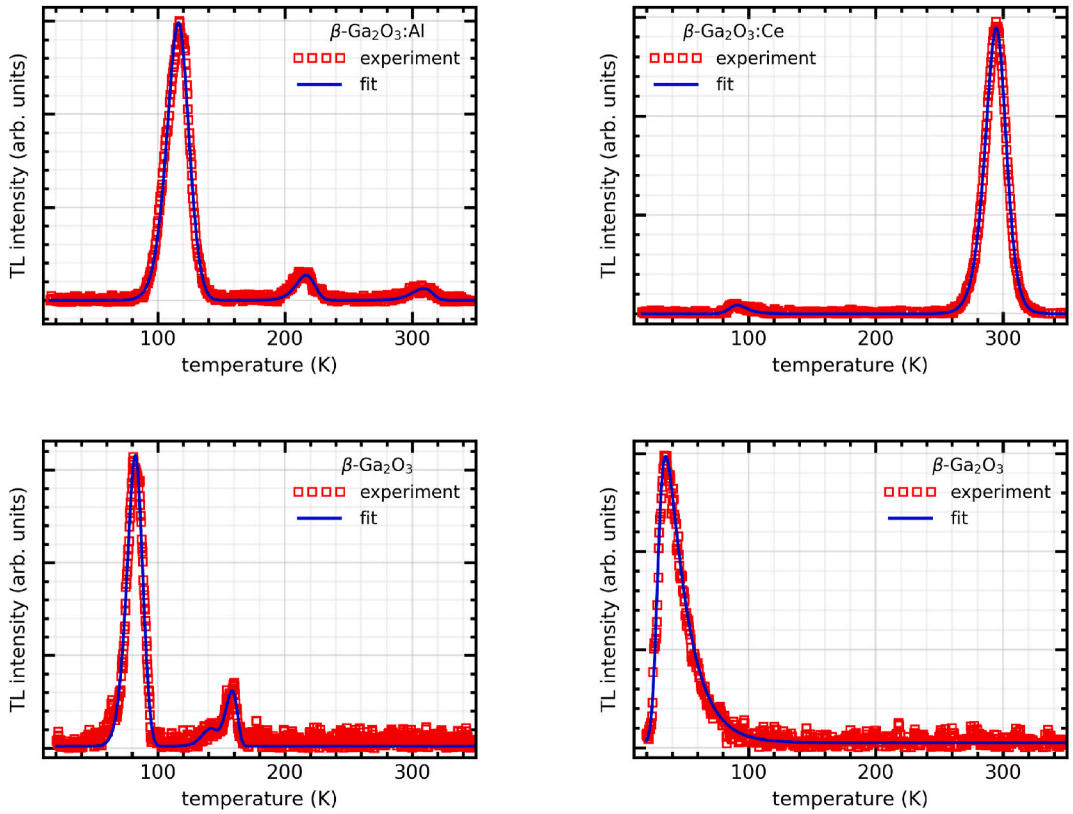

Fig. 3. Experimental and fitted glow curves of all samples from Table 1.

Table 2
Values of the trap parameters obtained with the fitting procedure.

ID	formula	$E_i + E_{qi}$ (meV)	σ^i_∞ (cm^2)	f_i	R_i
a	β-Ga_2O_3:Al (5.0%)	125	$6.31{\cdot}10^{-16}$	0.007	$1.41{\cdot}10^{4}$
		549	$8.91{\cdot}10^{-15}$	0.0007	$4.90{\cdot}10^{-4}$
		991	$7.94{\cdot}10^{-13}$	0.012	$5.89{\cdot}10^{-2}$
b	β-Ga_2O_3:Ce (0.1%)	173	$7.94{\cdot}10^{-16}$	0.4	$6.92{\cdot}10^{2}$
		1043	$2.51{\cdot}10^{-10}$	0.02	$1.45{\cdot}10^{-2}$
c	β-Ga_2O_3	85	$1.58{\cdot}10^{-17}$	0.003	$2.09{\cdot}10^{2}$
		279	$1.26{\cdot}10^{-16}$	0.00006	$1.62{\cdot}10^{-3}$
		427	$2.51{\cdot}10^{-14}$	0.005	$5.25{\cdot}10^{-3}$
d	β-Ga_2O_3	22.4	$2.00{\cdot}10^{-15}$	0.08	$2.57{\cdot}10^{6}$

The uncertainties of determination of E and σ are below 5%, while of f and R below 10%.

as well as to gallium vacancies [24].

For electrically insulating β-Ga_2O_3:Al (Fig. 3a) we observe three traps peaking at 115, 220, and 310 K, respectively. Their activation energies $E_i + E_{qi}$ obtained from the fitting procedure are 125, 549 and 991 meV. The corresponding cross sections σ^i_∞ are $6.31{\cdot}10^{-16}$ cm^2, $8.91{\cdot}10^{-15}$ cm^2 and $7.94{\cdot}10^{-13}$ cm^2. The initial filling of all these traps is very low. The retrapping process is dominating for the shallowest trap, as opposed to the two remaining traps.

The glow curve of electrically insulating β-Ga_2O_3:Ce (Fig. 3b) consists of two peaks located around 85 and 290 K. The parameters derived from the fitting procedure are 173 meV and $7.94{\cdot}10^{-16}$ cm^2, and 1043 meV and $2.51{\cdot}10^{-10}$cm^2, respectively. For the shallower trap retrapping prevails, which is not true for the deeper trap.

The undoped, electrically insulating β-Ga_2O_3 sample (Fig. 3c) shows in its ltTL two major peaks at 80 and 160 K, and one minor peak at 140 K. The corresponding depths are 85, 279, and 427 meV, and the cross sections are $3.98{\cdot}10^{-17}$, $1.58{\cdot}10^{-17}$ and $1.48{\cdot}10^{-13}$ cm^2, respectively. The relation between retrapping and recombination processes is similar as for β-Ga_2O_3:Al, i.e. retrapping dominates for the shallowest trap, contrary to the two remaining traps.

There is only one trap peaking around 35 K, with a depth of 23 meV and a cross section of $2.0{\cdot}10^{-15}$cm^2, identified by ltTL of the semiconducting β-Ga_2O_3 sample (Fig. 3d). Clearly, this trap is due to a partly compensated shallow donor, which is formed by Si and/or hydrogen [13]. The ionization energies of such donors assume values between 25 and 16 meV depending on the concentration and are limited by a value of 36 meV consistent with the effective-mass theory [21]. The trap depth of 23 meV fits well into this range of values. Not unexpectedly for the shallow effective-mass like donor, this trap has the highest ratio between retrapping and recombination. Generally, we notice that the process of retrapping is stronger in the shallower traps.

The nature of the remaining traps (with the sole exception of the trap peaking at about 300 K) identified in the three insulating samples, remains unclear. They may have become visible because of the lower Fermi level; in this case they could be due to some deep uncontrolled donor levels (such as iridium [28]) or are themselves responsible for the lowering of the Fermi level being some compensating deep acceptors (such as cobalt or magnesium [29]). The overall picture seems to be complex due to the presence of different impurities that interplay in between and with point defects.

The 300 K trap can be with a high probability associated with a deep compensating acceptor level of $Fe^{3+/2+}$, as proven directly by isothermal decays of photo-induced EPR signal of Fe^{2+} measured at temperatures between 290 and 310 K [30]. The 300 K TL glow peak is visible in two of the three insulating samples and, interestingly, for larger concentrations of Fe, the shallower traps are not populated (not present, or overwhelmed by Fe) during the irradiation phase in the ltTL measurement. We also note that the values of these trap depths from our fits at about 1 eV, are larger than the previously established value of about 0.7–0.8 eV [25,30] which, at the moment is not understood.

4. Conclusions

In this study, we have measured and characterized quantitatively low-temperature thermoluminescence of four β-Ga_2O_3 crystal samples. We have shown that the semi-insulating samples display much richer ltTL structure than the semiconducting one. The use of a rate equations model has allowed us to fit the glow curves and to determine the most important trap parameters. Concerning the nature of the detected traps, despite the complexity of the issue, we have presented some preliminary interpretations. Nevertheless, a further analysis is still necessary and will be published elsewhere.

CRediT authorship contribution statement

Marcin E. Witkowski: Conceptualization, Methodology, Investigation, Formal analysis, Software, Visualization, Writing – original draft. **Konrad J. Drozdowski:** Conceptualization, Methodology, Formal analysis, Software, Visualization, Writing – original draft. **Michał Makowski:** Investigation, Writing – review & editing. **Winicjusz Drozdowski:** Project administration, Methodology, Investigation, Writing – review & editing. **Andrzej J. Wojtowicz:** Methodology, Writing – review & editing. **Klaus Irmscher:** Resources, Methodology, Writing – review & editing. **Robert Schewski:** Resources, Investigation. **Zbigniew Galazka:** Conceptualization, Project administration, Resources, Methodology, Writing – review & editing.

Declaration of competing interest

The authors declare that they have no known competing financial interests or personal relationships that could have appeared to influence the work reported in this paper.

Data availability

Data will be made available on request.

Acknowledgements

This research has been financed from the funds of the Polish National Science Centre (NCN) and the German Research Foundation (DFG) in frames of a joint grant (NCN: 2016/23/G/ST5/04048, DFG:GA2057/2-1). The authors would like to thank Mike Pietsch (Leibniz-Institut für Kristallzüchtung) for measurements of electrical properties and Dr. Tobias Schulz (Leibniz-Institut für Kristallzüchtung) for critical reading of the present manuscript.:

References

[1] S.E. Derenzo, E. Bourret-Courshesne, G. Bizarri, A. Canning, Nucl. Instrum. Methods A805 (2016) 36–40.
[2] T. Yanagida, G. Okada, T. Kato, D. Nakauchi, S. Yanagida, APEX 9 (2016) 1–4, 042601.
[3] D. Szalkai, Z. Galazka, K. Irmscher, P. Tutto, A. Klix, D. Gehre, IEEE Trans. Nucl. Sci. 64 (2017) 1574–1579.
[4] N. He, H. Tang, B. Liu, Z. Zhu, Q. Li, C. Guo, M. Gu, J. Xu, J. Liu, M. Xu, L. Chen, X. Ouyang, Nucl. Instrum. Methods A888 (2018) 9–12.
[5] Z. Galazka, Semicond. Sci. Technol. 33 (2018) 113001/1–11300161.
[6] Y. Usui, D. Nakauchi, N. Kawano, G. Okada, N. Kawaguchi, T. Yanagida, J. Phys. Chem. Solid. 117 (2018) 36–41.
[7] W. Drozdowski, M. Makowski, M.E. Witkowski, A.J. Wojtowicz, K. Irmscher, R. Schewski, Z. Galazka, Opt. Mater. Express 11 (2021) 2488–2494.
[8] Z. Galazka, R. Schewski, K. Irmscher, W. Drozdowski, M.E. Witkowski, M. Makowski, A.J. Wojtowicz, I.M. Hanke, M. Pietsch, T. Schulz, D. Klimm, S. Ganschow, A. Dittmar, A. Fiedler, T. Schröder, M. Bickermann, J. Alloys Compd. 818 (2020) 152842/1–7.
[9] W. Drozdowski, M. Makowski, M.E. Witkowski, A.J. Wojtowicz, R. Schewski, K. Irmscher, Z. Galazka, Opt. Mater. 105 (2020) 109856/1–6.
[10] M.M. Islam, D. Rana, A. Hernandez, M. Haseman, F.A. Selim, J. Appl. Phys. 125 (2019) 1–9, 055701.
[11] A. Luchechko, V. Vasyltsiv, L. Kostyk, O. Tsvetkova, A.I. Popov, Nucl. Instrum. Methods B441 (2019) 12–17.
[12] W. Drozdowski, M. Makowski, M.E. Witkowski, A.J. Wojtowicz, Z. Galazka, K. Irmscher, R. Schewski, Radiat. Meas. 121 (2019) 49–53.
[13] Z. Galazka, K. Irmscher, R. Schewski, I.M. Hanke, M. Pietsch, S. Ganschow, D. Klimm, A. Dittmar, A. Fiedler, T. Schroeder, M. Bickermann, J. Cryst. Growth 529 (2020) 125297/1–8.
[14] A.J.J. Bos, Radiat. Meas. 41 (2006) S45–S56.
[15] J.T. Randall, M.H.F. Wilkins, Proc. Roy. Soc. Lond. A184 (1945) 366–407.
[16] S. McKeever, N. Agersnap Larsen, L. Bøtter-Jensen, V. Mejdahl, Radiat. Meas. 27 (1997) 75–82.
[17] R. Chen, S.W.S. McKeever, Theory of Thermoluminescence and Related Phenomena,", World Scientific, 1997.
[18] R. Chen, V. Pagonis, Nucl. Instrum. Methods B312 (2013) 60–69.
[19] K. Levenberg, Q. Appl. Math. 2 (1944) 164–168.
[20] D.W. Marquardt, J. Soc. Ind. Appl. Math. 11 (1963) 431–441.
[21] Z. Zhang, E. Farzana, A.R. Arehart, S.A. Ringel, Appl. Phys. Lett. 108 (2016) 1–5, 052105.
[22] Y. Nakano, ECS J. Solid State Sci. Technol. 6 (2017) 615–617.
[23] Z. Galazka, J. Appl. Phys. 131 (2022), 031103/1-03110322.
[24] M.E. Ingebrigtsen, J.B. Varley, A.Yu Kuznetsov, B.G. Svensson, G. Alfieri, A. Mihaila, U. Badstübner, L. Vines, Appl. Phys. Lett. 112 (2018) 1–5, 042104.
[25] K. Irmscher, Z. Galazka, M. Pietsch, R. Uecker, R. Fornari, J. Appl. Phys. 110 (2011) 1–7, 063720.
[26] A.Y. Polyakov, N.B. Smirnov, I.V. Shchemerov, E.B. Yakimov, J. Yang, F. Ren, G. Yang, J. Kim, A. Kuramata, S.J. Pearton, Appl. Phys. Lett. 112 (2018) 1–5, 032107.
[27] C.A. Lenyk, N.C. Giles, E.M. Scherrer, B.E. Kananen, L.E. Halliburton, K.T. Stevens, G.K. Foundos, J.D. Blevins, D.L. Dorsey, S. Mou, J. Appl. Phys. 125 (2019) 1–7, 045703.
[28] P. Seyidov, M. Ramsteiner, Z. Galazka, K. Irmscher, J. Appl. Phys. 131 (2022) 1–6, 035707.
[29] P. Seyidov, J.B. Varley, Z. Galazka, T.S. Chou, A. Popp, A. Fiedler, K. Irmscher, Apl. Mater. (2022) submitted for publication.
[30] C.A. Lenyk, T.D. Gustafson, L.E. Halliburton, N.C. Giles, J. Appl. Phys. 126 (2019) 245701/1–9.